Journal of Advanced Research 36 (2022) 63–71

Contents lists available at ScienceDirect

Journal of Advanced Research

journal homepage: www.elsevier.com/locate/jare

Propagation and interaction between special fractional soliton and soliton molecules in the inhomogeneous fiber

Gang-Zhou Wu [a], Chao-Qing Dai [a,*], Yue-Yue Wang [a], Yi-Xiang Chen [b]

[a] College of Sciences, Zhejiang A&F University, Lin'an, Zhejiang 311300, PR China
[b] School of Electronics Information, Zhejiang University of Media and Communications, Hangzhou 310018, PR China

HIGHLIGHTS

- Analytical chirp-free and chirped fractional soliton solutions are obtained.
- The form conditions of soliton molecules are given.
- Interactions between special fractional solitons and soliton molecules are discussed.

GRAPHICAL ABSTRACT

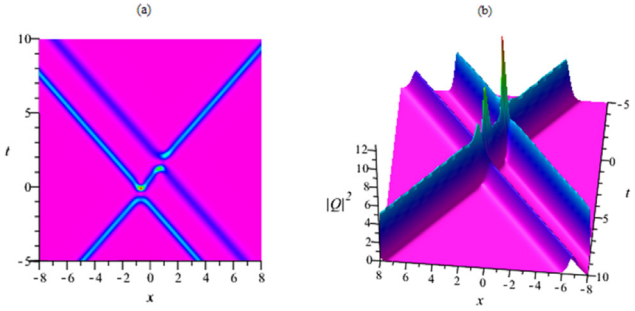

ARTICLE INFO

Article history:
Received 30 August 2020
Revised 8 May 2021
Accepted 12 May 2021
Available online 18 May 2021

Keywords:
Fractional nonlinear Schrödinger equation
Distributed coefficients
Interaction
Special soliton
Soliton molecules

ABSTRACT

Introduction: Fractional nonlinear models have been widely used in the research of nonlinear science. A fractional nonlinear Schrödinger equation with distributed coefficients is considered to describe the propagation of pi-second pulses in inhomogeneous fiber systems. However, soliton molecules based on the fractional nonlinear Schrödinger equation are hardly reported although many fractional soliton structures have been studied.
Objectives: This paper discusses the propagation and interaction between special fractional soliton and soliton molecules based on analytical solutions of a fractional nonlinear Schrödinger equation.
Methods: Two analytical methods, including the variable-coefficient fractional mapping method and Hirota method with the modified Riemann–Liouville fractional derivative rule, are used to obtain analytical non-travelling wave solutions and multi-soliton approximate solutions.
Results: Analytical non-travelling wave solutions and multi-soliton approximate solutions are derived. The form conditions of soliton molecules are given, and the dynamical characteristics and interactions between special fractional solitons, multi-solitons and soliton molecules are discussed in the periodic inhomogeneous fiber and the exponential dispersion decreasing fiber.
Conclusion: Analytical chirp-free and chirped non-traveling wave solutions and multi-soliton approximate solutions including soliton molecules are obtained. Based on these solutions, dynamical characteristics and interactions between special fractional solitons, multi-solitons and soliton molecules are discussed. These theoretical studies are of great help to understand the propagation of optical pulses in fibers.

© 2021 The Authors. Published by Elsevier B.V. on behalf of Cairo University.

Peer review under responsibility of Cairo University.
* Corresponding author.

https://doi.org/10.1016/j.jare.2021.05.004
2090-1232/© 2021 The Authors. Published by Elsevier B.V. on behalf of Cairo University.

Introduction

A soliton is known as a self-reinforcing wave packet that keeps its shape and propagating velocity. Soliton exhibits its rich structures including optical soliton [1], plane soliton [2], soliton molecules [3], rogue waves [4], etc., and helps develop some breakthrough branches of physical sciences [5-7] such as optics, condense physics, fluid and plasma [8-11].

Soliton molecules mean robust multi-soliton bound states [12], and their dynamics have become hot topics in several contexts, including optical systems [13,14] and Bose–Einstein condensates [15]. The formation of optical soliton molecules originates from the existence of attractors of a nonlinear dynamical system. Once formed, soliton molecules will stably travel around a mode-locked laser cavity [14]. For a soliton molecule, temporal separations among solitons are the most relevant degrees of freedom [13]. The real-time internal dynamics of two-soliton and three-soliton molecules were experimentally studied [14,16]. Optical soliton molecular complexes have been experimentally observed in a passively mode-locked fiber laser [17]. The breathing soliton molecules were also experimentally found in a mode-locked fiber laser [18].

These studies above focused on experimental observations [12-18]. However, theoretical investigation on soliton molecules was less carried out. Until fairly recently, the formation mechanism of soliton molecules was theoretically proposed [3,19-21]. Soliton molecules based on fractional nonlinear models(FNMs) are hardly reported although many fractional soliton structures have been studied [22,23].

In recent years, FNMs have been widely used in the research of nonlinear science [24-26]. At the same time, FNMs with distributed coefficients have certain representative significance. Many phenomena can be described successfully by using FNMs such as plasma, nonlinear optics and chaotic oscillations [24]. Many researchers have already succeeded in the study of fractional models [27,29]. Effective methods for solving fractional nonlinear Schrödinger (FNLS) equation have been achieved [30], such as the fractional F-expansion method [28], fractional Riccati method [26] and fractional bi-function method [31]. At the same time, some numerical methods have also been successfully used to solve the fractional nonlinear Schrodinger equation [32], and numerical solutions were derived by using Riesz-Feller Derivative and non-standard discretization [33,34]. These numerical methods have been validated by the researchers [35].

The novelty of this paper lies in presenting a new strategy to get analytical fractional non-travelling wave solution and multi-soliton solutions of a FNLS equation by altogether utilizing fractional mapping method and Hirota method with the modified Riemann–Liouville(RL) fractional derivative rule. Another novelty is to study the dynamics of special fractional soliton and soliton molecules, and discuss the formation mechanism of soliton molecules. The stability of the special fractional soliton and soliton molecule is analyzed through a series of numerical studies. These conclusions possess theoretical guidance for the related experimental study in all-optical switches, optical amplifier and mode-locked lasers.

Material and methods

To our knowledge, most practical nonlinear physical models have distributed coefficients. For example, modern communication systems use variable dispersion fiber. The NLS equation with distributed coefficients can describe the propagation of pi-second pulses in inhomogeneous fiber systems [38,39]. Recently, many scholars believe that the evolution of the development function can be well described by FNMs. When describing practical problems, compared with the integer model, FNMs are more satisfactory [36]. The FNLS equation with distributed coefficients was introduced as [37]

$$iD_x^{\lambda}Q+\frac{1}{2}\alpha(x)D_t^{2\mu}Q+\beta(x)Q|Q|^2-i\rho(x)Q=0, 0<\lambda,\mu\leqslant 1, x>0, \tag{1}$$

where the complex envelope $Q=Q(x,t)$and its derivatives $D_x^{\lambda}Q=\partial^{\lambda}Q/\partial x^{\lambda}, D_t^{2\mu}Q=\partial^{2\mu}Q/\partial t^{2\mu}$

with the fractional orders $\lambda$and μ, the delay time t and longitudinal propagation distance x. Functions$\beta(x)$and$\alpha(x)$are coefficients of the Kerr nonlinearity and dispersion, and function $\rho(x)$is adiabatic amplification (loss) for $\rho(x)<0$ or gain for $\rho(x)>0$. If $\lambda=\mu=1$, Eq. (1) is the variable-coefficient NLS equation [38]. When functions$\beta(x)$and$\alpha(x)$are constant and $\rho(x)=0$, Eq. (1) describe solitons in the homogeneous fiber [39]. Here the modified RL fractional derivative is defined as [40]

$$D_x^{\lambda}f(x)=\begin{cases}\frac{1}{\Gamma(-\lambda)}\int_0^x(x-\psi)^{-\lambda-1}[f(\psi)-f(0)]d\psi\ \lambda<0\\ \frac{1}{\Gamma(1-\lambda)}\frac{d}{dx}\int_0^x(x-\psi)^{-\lambda}[f(\psi)-f(0)]d\psi\ 0<\lambda<1\\ [f^{(\lambda-a)}(x)]^{(a)}\ a\geqslant 1, a\leqslant\lambda<a+1\end{cases} \tag{2}$$

they has the following properties [41,42]

$$\begin{aligned}D_x^{\lambda}x^{\gamma}&=\tfrac{\Gamma(\gamma+1)}{\Gamma(\gamma+1-\lambda)}x^{\gamma-\lambda},\ \gamma>0,\\ D_x^{\lambda}(ca(x))&=cD_x^{\lambda}a(x), with\, c=const,\\ D_x^{\lambda}(a(x)b(x))&=\sigma_x\{a(x)D_x^{\lambda}b(x)+b(x)D_x^{\lambda}a(x)\},\\ D_x^{\lambda}a[b(x)]&=\sigma_x a'_b[b(x)]D_x^{\lambda}b(x),\\ D_x^{\lambda}a[b(x)]&=\sigma_x D_b^{\lambda}a[b(x)](b'_x)^{\lambda},\end{aligned} \tag{3}$$

with the following inequality [42]

$$D_x^{\lambda}a(x)\cong\Gamma(\lambda+1)D_x a(x) \tag{4}$$

In Eq. (3), the fractal index σ_x is usually calculated from a gamma function. Abdel-Salam et al. found that for the Mittag-Leffler function as $V_{\lambda}(x)=\sum_{l=0}^{\infty}x^l/\Gamma(1+l\lambda), \lambda>0$, the value of the fractal index is equal to one [42].

Analytical non-travelling wave solutions of FNLS equation (1)

We suppose that Eq.(1) has the form of the following solution

$$Q=qV_{\lambda}(i\phi^{\lambda}), \phi=k(x)t^2+m(x)t+n(x), \tag{5}$$

where the amplitude $q=q(x,t)$, chirped phase$k(x)$,linear phase$m(x)$ and phase shift $n(x)$ are functions of $\times$, making $\lambda=\mu$, separating the imaginary and real parts, thus

$$\begin{aligned}&\alpha(x)kqV_{\lambda}(i\phi^{\lambda})+\alpha(x)(2kt+m)^{\lambda}V_{\lambda}(i\phi^{\lambda})D_t^{\lambda}q-\rho(x)qV_{\lambda}(i\phi^{\lambda})\\ &+V_{\lambda}(i\phi^{\lambda})D_x^{\lambda}q\\ &=0,\end{aligned} \tag{6}$$

$$\begin{aligned}&-(k_xt^2+m_xt+n_x)^{\lambda}qV_{\lambda}(i\phi^{\lambda})-\tfrac{1}{2}\alpha(x)(2kt+m)^{2\lambda}qV_{\lambda}(i\phi^{\lambda})+\tfrac{1}{2}\alpha(x)D_t^{2\lambda}qV_{\lambda}(i\phi^{\lambda})\\ &+\beta(x)q^3V_{\lambda}(i\phi^{\lambda})V_{\lambda}(-i\phi^{\lambda})V_{\lambda}(i\phi^{\lambda})=0\end{aligned} \tag{7}$$

We suppose that Eqs. (6) and (7) have following solution

$$q(x,t)=g_0+\sum_{e=1}^{l}[g_eY^e(\psi)+f_eY^{-e}(\psi)], \tag{8}$$

where $g_0 = g_0(x), g_e = g_e(x), f_e = f_e(x), (e = 1, ..., l)$are functions of $\times$, $\psi = \psi(x,t)$is a function of $\times$ and t,$\psi = r(x)t + s(x)$with group velocity $s(x)$and pulse width $r(x)$are functions of $\times$, by the leading term analysis in Eq. (7) can get $l = 1$. Here $Y(\psi)$satisfies the fractional mapping equation [28]

$$D_{\Psi}^{\lambda}Y = \sqrt{a_0 + a_2Y^2 + a_4Y^4}, \tag{9}$$

with arbitrary constants a_0, a_2, a_4. Eq. (9) has different forms of solutions listed in Table 1.

In table 1, the extended hyperbolic and trigonometric functions satisfy the following definitions

$$\begin{gathered}\sinh(\psi,\lambda) = \tfrac{1}{2}(V_\lambda(\psi^\lambda) - V_\lambda(-\psi^\lambda)), \cosh(\psi,\lambda) = \tfrac{1}{2}(V_\lambda(\psi^\lambda) + V_\lambda(-\psi^\lambda)),\\ \cos(\psi,\lambda) = \tfrac{1}{2}(V_\lambda(i\psi^\lambda) + V_\lambda(-i\psi^\lambda)), \sin(\psi,\lambda) = \tfrac{1}{2i}(V_\lambda(i\psi^\lambda) - V_\lambda(-i\psi^\lambda)),\\ \tanh(\psi,\lambda) = \tfrac{\sinh(\psi,\lambda)}{\cosh(\psi,\lambda)}, sech(\psi,\lambda) = \tfrac{1}{\cosh(\psi,\lambda)}, \tan(\psi,\lambda) = \tfrac{\sin(\psi,\lambda)}{\cos(\psi,\lambda)}, \sec(\psi,\lambda) = \tfrac{1}{\cos(\psi,\lambda)}.\end{gathered} \tag{10}$$

Substituting ansatz (8) with $l = 1$and (9) into Eqs. (6) and (7), considering the approximation of the generalized binomial theorem, and making the coefficients of $t^cY^d(c = 0,1,2, d = 0,1,2,3)$and $\sqrt{a_0 + a_2Y^2 + a_4Y^4}$ zero get

$$\begin{gathered}g_i(\alpha k^{2\lambda} + 2(k_x)^\lambda) = 0, g_i(4\alpha m^\lambda k^\lambda + 2(m_x)^\lambda) = 0,\\ 2\alpha r^2 a_4 g_2 + 2Mg_2^3\beta = 0, 6Mg_1g_j^2 = 0,\\ g_j\alpha m^{2\lambda} - g_j\alpha r^2 a_2 - 6Mg_1^2g_j\beta - 6Mg_2^2g_3\beta + 2g_jn_x^\lambda = 0,\\ 2Mg_1^3\beta + 12Mg_1g_2g_3 - g_1\alpha m^{2\lambda} - 2g_1(n_x)^\lambda = 0,\\ g_j(\alpha rk^\lambda + D_x^\lambda r) = 0, 2D_x^\lambda g_i - 2\rho g_i + \alpha k g_i = 0,\\ 2\alpha r^2 a_0 g_3 + 2Mg_3^3\beta = 0, g_j(\alpha rm^\lambda + D_x^\lambda s) = 0.\end{gathered} \tag{11}$$

where $M = V_\lambda(-i\phi^\lambda)V_\lambda(i\phi^\lambda)$ with $(i = 1,2,3, j = 2,3)$.

Solving Eqs. (11), using Eqs. (5) and (8) with solutions in Table 1, we can get several families of solutions of Eq. (1). Due to the limit of length, we only list part of solutions.

Family 1. when $a_0 = 1, a_2 = -2, a_4 = 1$,

(I) Fractional chirp-free dark soliton solution

$$Q_{11} = C_3V_\lambda[\int_0^x \rho(\xi)(d\xi)^\lambda]\tanh(\psi,\lambda)V_\lambda\{i[C_1t + \int_0^x \sqrt[\lambda]{\frac{1}{2}(-2C_2^2 - C_1^{2\lambda})\alpha(\xi)}d\xi + C_5]^\lambda\}, \tag{12}$$

where

$\psi = C_2t - C_1{}^\lambda C_2\Gamma^{-1}(\lambda)\int_0^x (x-\xi)^{\lambda-1}\alpha(\xi)d\xi + C_4, \beta = -\frac{\alpha C_2^2\{V_\lambda[\int_0^x \rho(\xi)(d\xi)^\lambda]\}^{-2}}{MC_3^2}$.$\rho(x)and\alpha(x)$are functions of $x$and C_1~C_5 are arbitrary constants.

(II) Fractional chirp-free combined soliton solution

$$\begin{aligned}Q_{12} = C_3V_\lambda[&\int_0^x \rho(\xi)(d\xi)^\lambda][\tanh(\psi,\lambda)\\ &\pm \coth(\psi,\lambda)]V_\lambda\{i[C_1t + n(x)]^\lambda\},\end{aligned} \tag{13}$$

where

$\psi = C_2t - C_1{}^\lambda C_2\Gamma^{-1}(\lambda)\int_0^x (x-\xi)^{\lambda-1}\alpha(\xi)d\xi + C_4, \beta = -\frac{\alpha C_2^2\{V_\lambda[\int_0^x \rho(\xi)(d\xi)^\lambda]\}^{-2}}{MC_3^2}$,
$n = \int_0^x \sqrt[\lambda]{[\frac{1}{2}(-2C_2^2 - C_1^{2\lambda}) \mp 3C_2^2]\alpha(\xi)}d\xi + C_5$,
$\rho(x)$ and $\alpha(x)$are functions of $x$and C_1~C_5 are arbitrary constants.

(III) Fractional chirped dark soliton solution

$$\begin{aligned}Q_{13} = C_3V_\lambda\{&\int_0^x [\rho(\xi)\\ &+ \frac{(k_\xi)^\lambda(\xi)}{2k^{2\lambda-1}(\xi)}](d\xi)^\lambda\}\tanh(\psi,\lambda)V_\lambda(i[kt^2 + C_1kt + n]^\lambda),\end{aligned} \tag{14}$$

where

$\alpha = -\frac{(k_x)^\lambda}{2k^{2\lambda}}, \psi = C_2V_\lambda[\int_0^x \frac{(k_\xi)^\lambda(\xi)}{k^\lambda(\xi)}(d\xi)^\lambda]t + C_1{}^\lambda\Gamma^{-1}(\lambda)\int_0^x (x-\xi)^{\lambda-1}\frac{(k_\xi)^\lambda(\xi)}{2k^\lambda(\xi)}r(\xi)d\xi + C_4,$
$\beta = -\frac{\alpha C_2^2\left\{V_\lambda[\int_0^x \frac{(k_\xi)^\lambda(\xi)}{k^\lambda(\xi)}(d\xi)^\lambda]\right\}^2}{MC_3^2\left\{V_\lambda[\int_0^x (\rho(\xi) + \frac{(k_\xi)^\lambda(\xi)}{2k^{2\lambda-1}(\xi)})(d\xi)^\lambda]\right\}^2}, n = \int_0^x \sqrt[\lambda]{\frac{1}{2}(-2r^2 - C_1^{2\lambda}k^{2\lambda})\alpha(\xi)}d\xi + C_5.$

$\rho(x)$ and $k(x)$are functions of $x$and C_1~C_5 are arbitrary constants.

(IV) Fractional chirped combined soliton solution

$$Q_{14} = C_3V_\lambda\left\{\int_0^x \left[\rho(\xi) + \frac{(k_\xi)^\lambda(\xi)}{2k^{2\lambda-1}(\xi)}\right](d\xi)^\lambda\right\}\{\tanh(\psi,\lambda) \pm \coth(\psi,\lambda)\}V_\lambda\left(i[kt^2 + C_1kt + n]^\lambda\right) \tag{15}$$

where

$\alpha = -\frac{(k_x)^\lambda}{2k^{2\lambda}}, \psi = C_2V_\lambda\left[\int_0^x \frac{(k_\xi)^\lambda(\xi)}{k^\lambda(\xi)}(d\xi)^\lambda\right]t + C_1{}^\lambda\Gamma^{-1}(\lambda)\int_0^x (x-\xi)^{\lambda-1}\frac{(k_\xi)^\lambda(\xi)}{2k^\lambda(\xi)}r(\xi)d\xi + C_4,$
$n = \int_0^x \sqrt[\lambda]{\left[\frac{1}{2}(-2r^2 - C_1^{2\lambda}k^{2\lambda}) \mp 3r^2\right]\alpha(\xi)}d\xi + C_5, \beta = -\frac{\alpha C_2^2\left\{V_\lambda\left[\int_0^x \frac{(k_\xi)^\lambda(\xi)}{k^\lambda(\xi)}(d\xi)^\lambda\right]\right\}^2}{MC_3^2\left\{V_\lambda\left[\int_0^x (\rho(\xi) + \frac{(k_\xi)^\lambda(\xi)}{2k^{2\lambda-1}(\xi)})(d\xi)^\lambda\right]\right\}^2}.$

$\rho(x)$ and $k(x)$ are functions of $x$and C_1~C_5 are arbitrary constants.

Family 2. when $a_0 = 0, a_2 = 1, a_4 = -1$,

(I) Fractional chirp-free bright soliton solution

$$Q_{21} = C_3V_\lambda[\int_0^x \rho(\xi)(d\xi)^\lambda]sech(\psi,\lambda)V_\lambda\{i[C_1t + \int_0^x \sqrt[\lambda]{\frac{1}{2}(C_2^2 - C_1^{2\lambda})\alpha(\xi)}d\xi + C_5]^\lambda\}, \tag{16}$$

where

$\psi = C_2t - C_1{}^\lambda C_2\Gamma^{-1}(\lambda)\int_0^x (x-\xi)^{\lambda-1}\alpha(\xi)d\xi + C_4, \beta = \frac{\alpha C_2^2\{V_\lambda[\int_0^x \rho(\xi)(d\xi)^\lambda]\}^{-2}}{MC_3^2}$.

(II) Fractional chirped bright soliton solution

$$\begin{aligned}Q_{22} = C_3V_\lambda\{&\int_0^x [\rho(\xi)\\ &+ \frac{(k_\xi)^\lambda(\xi)}{2k^{2\lambda-1}(\xi)}](d\xi)^\lambda\}sech(\psi,\lambda)V_\lambda(i[kt^2 + C_1kt + n]^\lambda),\end{aligned} \tag{17}$$

where

Table 1
Some solutions of Eq. (9).

Case	a_0	a_2	a_4	Y
1	1	−2	1	$Y = \tanh(\psi,\lambda)$
2	0	1	−1	$Y = sech(\psi,\lambda)$
3	1/4	−1/2	1/4	$Y = \frac{\tanh(\psi,\lambda)}{1\pm sech(\psi,\lambda)}, Y = \coth(\psi,\lambda) + csch(\psi,\lambda), Y = \tanh(\psi,\lambda) + isech(\psi,\lambda)$
4	0	1	1	$Y = csch(\psi,\lambda)$
5	1	1	0	$Y = \sinh(\psi,\lambda)$
6	−1	1	0	$Y = \cosh(\psi,\lambda)$
7	1	−1	0	$Y = \sin(\psi,\lambda), Y = \cos(\psi,\lambda)$
8	0	−1	1	$Y = \csc(\psi,\lambda), Y = \sec(\psi,\lambda)$
9	1	2	1	$Y = \cot(\psi,\lambda), Y = \tan(\psi,\lambda)$

$$\alpha=-\frac{(k_x)^{\lambda}}{2k^{2\lambda}},\psi=C_2V_{\lambda}\left[\int_0^x\frac{(k_\xi)^{\lambda}(\xi)}{k^{\lambda}(\xi)}(d\xi)^{\lambda}\right]t+C_1{}^{\lambda}\Gamma^{-1}(\lambda)\int_0^x(x-\xi)^{\lambda-1}\frac{(k_\xi)^{\lambda}(\xi)}{2k^{\lambda}(\xi)}r(\xi)d\xi+C_4,$$

$$\beta=\frac{\alpha C_2^2\left\{V_{\lambda}\left[\int_0^x\frac{(k_\xi)^{\lambda}(\xi)}{k^{\lambda}(\xi)}(d\xi)^{\lambda}\right]\right\}^2}{MC_3^2\left\{V_{\lambda}\left[\int_0^x(\rho(\xi)+\frac{(k_\xi)^{\lambda}(\xi)}{2k^{2\lambda-1}(\xi)}(d\xi)^{\lambda}\right]\right\}^2},n=\int_0^x\sqrt[\lambda]{\frac{1}{2}(r^2-C_1^{2\lambda}k^{2\lambda})\alpha(\xi)}d\xi+C_5.$$

Multi-soliton approximate solutions of FNLS equation (1)

In order to study the dynamics of multi-soliton solutions, we use the inequality (4) in Eq.(1), thus Eq.(1) is converted into

$$i\Gamma(\lambda+1)D_xQ+\frac{1}{2}\alpha(x)\Gamma(\lambda+1)^2D_{tt}Q+\beta(x)Q|Q|^2-i\rho(x)Q=0,x>0,0<\lambda\leqslant 1. \tag{18}$$

Because the approximate expression (4) is used here, thus we call these solutions derived in the following as approximate solutions. Similar to the solving procedure in Section 3, we can also derive fractional bright and dark soliton approximate solution with and without chirped phase by using the fractional mapping method. For the limit of length, we do not list them.

Using the Hirota method, we can get a chirp-free bright soliton approximate solution like that derived from the fractional mapping method. However, we can not get chirped bright soliton approximate solution.

Next, we will get chirp-free multi-soliton approximate solution. From the Hirota method [43], we assume that $Q=e^{\frac{1}{\Gamma(\lambda+1)}\int\rho(x)dx}h(x,t)/f(x,t)$,where $h(x,t)$is complex function, and $f(x,t)$is real function. We get the bilinear equation of Eq. (18) as follows

$$2iD_xh\cdot f+\Gamma(\lambda+1)^2\alpha(x)D_t^2h\cdot f=0, \tag{19}$$

$$2\beta(x)e^{\frac{2}{\Gamma(\lambda+1)}\int\rho(x)dx}h\cdot h^*-\Gamma(\lambda+1)^2\alpha(x)D_t^2f\cdot f=0, \tag{20}$$

where * denotes the complex conjugate, D_x and D_t are Hirota bilinear operator. In order to solve Eqs. (19), (20), we can write $h(x,t)$ and $f(x,t)$ as power series expansions [43,44]

$$\begin{aligned}h(x,t)&=\varepsilon h_1(x,t)+\varepsilon^3h_3(x,t)+\varepsilon^5h_5(x,t)+\cdots,\\ f(x,t)&=1+\varepsilon^2f_2(x,t)+\varepsilon^4f_4(x,t)+\varepsilon^6f_6(x,t)+\cdots.\end{aligned} \tag{21}$$

Two soliton solutions via the Hirota method

In order to get the two soliton solution, we suppose that Eq. (18) has a solution as

$$\begin{aligned}h(x,t)&=h_1(x,t)+h_3(x,t),\\ f(x,t)&=1+f_2(x,t)+f_4(x,t),\end{aligned} \tag{22}$$

where

$$h_1(x,t)=e^{\theta_1}+e^{\theta_2}, \tag{23}$$

with$\theta_j=a_j(x)+s_jt+k_j=a_{j1}(x)+ia_{j2}(x)+(s_{j1}+is_{j2})t+k_{j1}+ik_{j2}$. Here$s_{j1}$,$s_{j2}$,$k_{j1}$ and$k_{j2}$are real numbers related to the group velocity, phase velocity, soliton position and phase of the j-th soliton respectively, $a_{j1}(x)$and $a_{j2}(x)$are pending functions. Substituting $h_1(x,t)$into Eq. (19), collect the coefficient of ε, we get $a_{j1}(x)$and$a_{j2}(x)$.

Substituting $h_1(x,t)$into Eq. (19), collect the coefficient of ε^2, we get

$$f_2=G_1e^{\theta_1+\theta_1{}^*}+G_2e^{\theta_2+\theta_1{}^*}+G_3e^{\theta_1+\theta_2{}^*}+G_4e^{\theta_2+\theta_2{}^*} \tag{24}$$

where $G_1=A_1$, $G_2=A_4$, $G_3=A_2$, $G_4=A_5$, $K$is an arbitrary constant.

Substituting $h_1(x,t)$and $f_2(x,t)$into Eq.(19), collect the coefficient of ε^3 , we get

$$h_3=G_5e^{\theta_1+\theta_2+\theta_1^*}+G_6e^{\theta_1+\theta_2+\theta_2^*} \tag{25}$$

where $G_5=B_1$,$G_6=B_2$

Substituting $h_1(x,t)f_2(x,t)$and $h_3(x,t)$ into Eq.(20), collect the coefficient of ε^4, we get

$$f_4=G_7e^{\theta_1+\theta_2+\theta_1^*+\theta_2^*}, \tag{26}$$

where $G_7=M_1$

We assume that $\varepsilon=1$, we get the two soliton solution

$$Q=\frac{h(x,t)}{f(x,t)}=\frac{h_1(x,t)+h_3(x,t)}{1+f_2(x,t)+f_4(x,t)}, \tag{27}$$

where $h_1(x,t)$, $h_3(x,t)$, $f_2(x,t)$and $f_4(x,t)$ are given in Eqs.(23), (24)-(26). We list coefficients $A_1,A_2,A_4,A_5,B_1,B_2,M_1$of Eq.(27) in Appendix A.

Three soliton solutions via the Hirota method

In order to get the three soliton solution, we assume that Eq. (18) has a solution as [43]

$$\begin{aligned}h(x,t)&=h_1(x,t)+h_3(x,t)+h_5(x,t),\\ f(x,t)&=1+f_2(x,t)+f_4(x,t)+f_6(x,t),\end{aligned} \tag{28}$$

using the similar steps in Section 4.1, we can define $\varepsilon=1$, we can get the three soliton solution of Eq. (18)

$$Q=\frac{h(x,t)}{f(x,t)}=\frac{h_1(x,t)+h_3(x,t)+h_5(x,t)}{1+f_2(x,t)+f_4(x,t)+f_6(x,t)}e^{\frac{1}{\Gamma(\lambda+1)}\int\rho(x)dx}, \tag{29}$$

where parameters $h_1(x,t),h_3(x,t),h_5(x,t),f_2(x,t),f_4(x,t),\ f_6(x,t)$are listed in Appendix A.

Results & discussion

Based on analytical solutions (12)-(17) (27) and (29), some special fractional soliton, multi-soliton and soliton molecules can be constructed. When the order of the fractional soliton equals one, the fractional soliton becomes a traditional integer soliton, especially two soliton and three soliton solutions are similar to those solutions in Refs. [40,41].

In order to facilitate the study of the dynamic characteristics of the soliton, we select the exponential distributed control system [45]

$$\alpha(x)=\alpha_0\exp(-\sigma x)(\mathrm{Y}_0+\mathrm{Y}_1\sin(\delta x)), \tag{30}$$

where parameters $\alpha_0>0,\sigma$ and Y_1describe the group velocity dispersion. Particularly, if $\mathrm{Y}_1=0$, system (30) depicts the exponentially dispersion decreasing fiber [46]. If $\sigma=0$, system (30) depicts the periodic inhomogeneous fiber [47].

Special fractional soliton

The evolution of fractional chirp-free bright-type soliton solution (16) with different values of fractional orders versus $\times$ and t is shown in the periodic inhomogeneous fiber system in Figs. 1 and 2.The amplitude and the velocity of the bright soliton depend on $C_3V_{\lambda}[\int_0^x\rho(\xi)(d\xi)^{\lambda}]$ and $C_1^{\lambda}\alpha(x)$respectively, the phase shift is determined by$(C_2^2-C_1^{2\lambda})\alpha(\xi)/2$, and the time shift is related to$C_1^{\lambda}\int_0^x(x-\xi)^{\lambda-1}\alpha(\xi)d\xi$. We find that the dynamic characteristics of soliton are affected by different values of the fractional orderλ. When the value of fractional order$\lambda$is closer to 1, solution (16) describes the classic bright soliton in Fig. 1(a), where the amplitude gradually decreases due to $\rho(x)<0$. When$\lambda=0.5$, the amplitude of the soliton decreases rapidly and then tends to be fixed magnitude in Fig. 1(b). By comparing Fig. 2(a) with Fig. 2(b), we can find that the position of the soliton on the t-axis changes, which means that the soliton has a phase shift. When the value

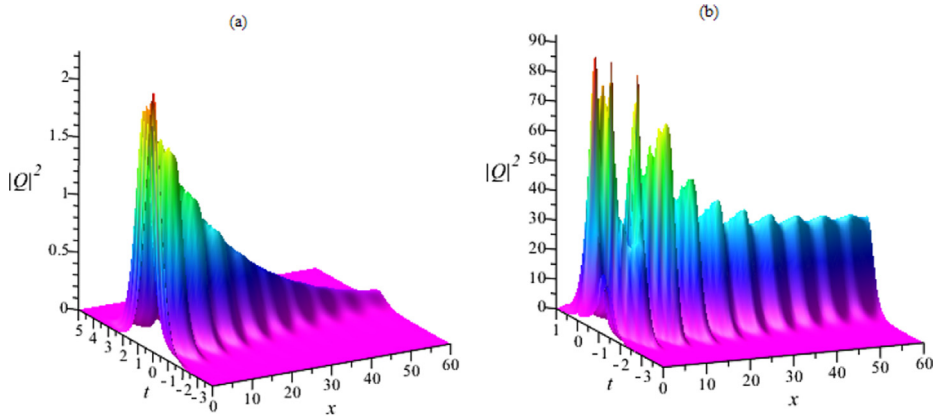

Fig. 1. Chirp-free bright soliton (16) with the intensity$|Q|^2$. Parameters are $C_1 = 0.8, C_2 = C_3 = 1.5, C_4 = C_5 = 0, \alpha(x) = \exp(-0.05x)\sin(x), \rho(x) = -0.025$with (a) $\lambda = 1$and (b) $\lambda = 0.5$

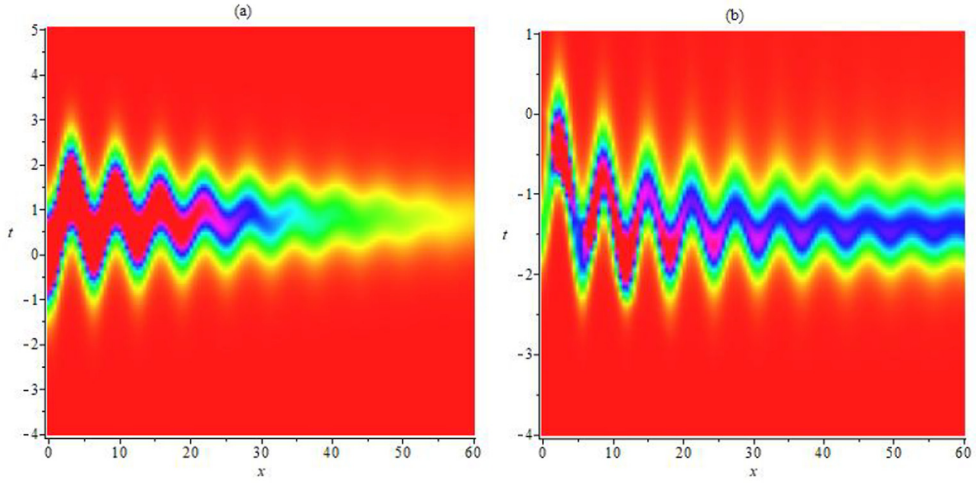

Fig. 2. Density map of chirp-free bright soliton $|Q_{21}|^2$. Parameters are same as Fig. 1.

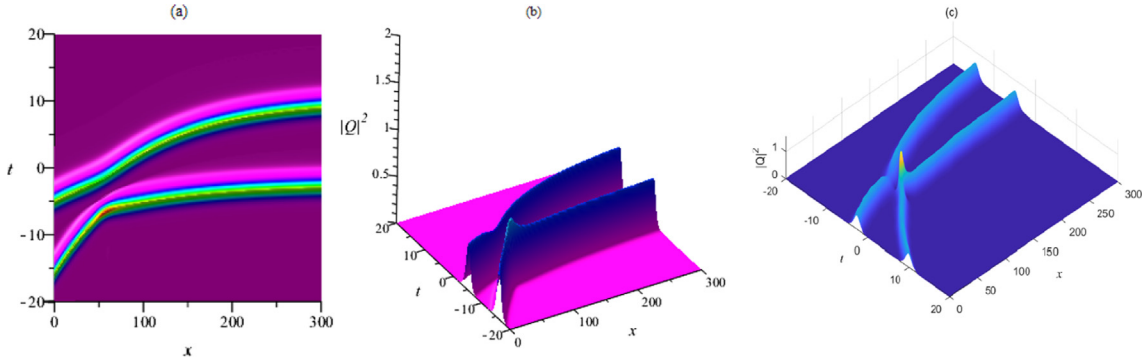

Fig. 3. The dynamical interaction of the two-soliton solution: (a) density plot, (b) intensity plot and (c) numerical rerun with 5% white random noise. Parameters are$s_{11} = s_{21} = 1, s_{12} = 0.3, s_{22} = 0.1, k_{11} = -5, k_{12} = 2, k_{21} = 3, k_{22} = -2, \lambda = 0.5, P = 2, \rho(x) = 0, \alpha(x) = 0.8\exp(-0.01x)$.

of fractional order $\lambda$is closer to 0.5, the periodicity of the soliton is significantly weakened. It can be clearly seen that the propagation speed of the soliton along the fiber has changed due to the presence of the parameter C_1. This shows that the soliton keeps its -sech-function shape even if the velocity is changed. This is an important property of solitons.

Multi-soliton and soliton molecules

The interaction of the two-soliton solution (27) in the exponential system is shown in Fig. 3. The two solitons continue to move after elastic collision, and their shape remain unchanged. By changing the parameters of phase velocity s_{12}ands_{22}, we can con-

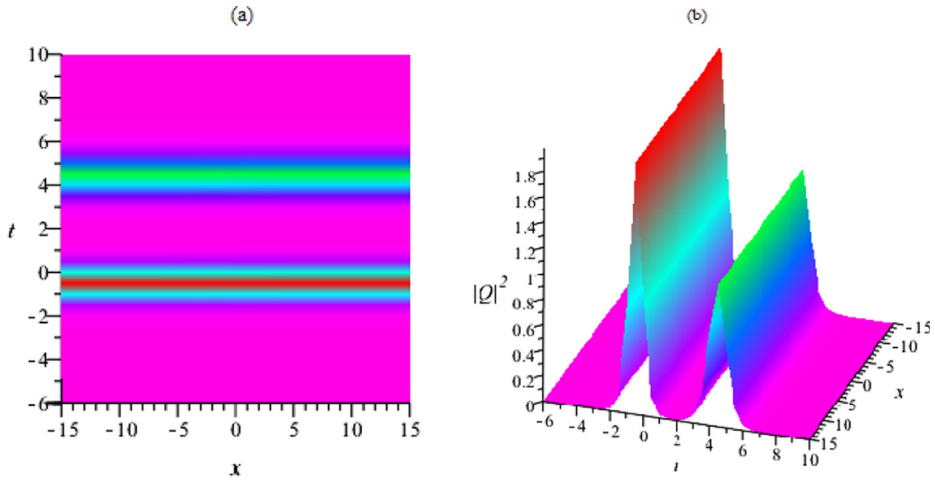

Fig. 4. A soliton molecule consisting of two solitons: (a) density plot and (b) intensity plot. Parameters are$s_{11} = 1.5, s_{12} = -0.3, s_{21} = 2, s_{22} = -0.3, k_{11} = -2, k_{12} = -2, k_{21} = 2, k_{22} = -2, \lambda = 0.5, P = 2, \rho(x) = 0, \alpha(x) = 0.0034\exp(-0.076x)$.

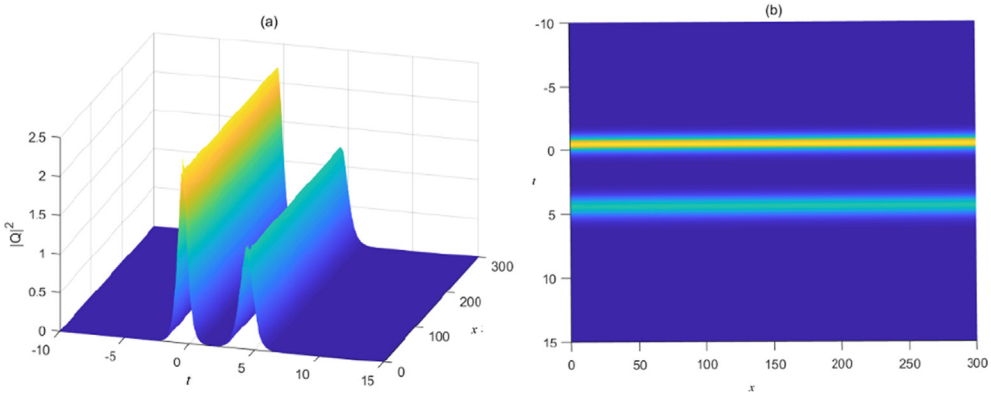

Fig. 5. The numerical rerun of the soliton molecule in Fig. 4 with 5% white random noise: (a) intensity plot and (b) density plot. Parameters are $s_{11} = 1.5, s_{12} = -0.3, s_{21} = 2, s_{22} = -0.3, k_{11} = -2, k_{12} = -2, k_{21} = 2, k_{22} = -2, \lambda = 0.5, P = 2, \rho(x) = 0, \alpha(x) = 0.0034\exp(-0.076x)$

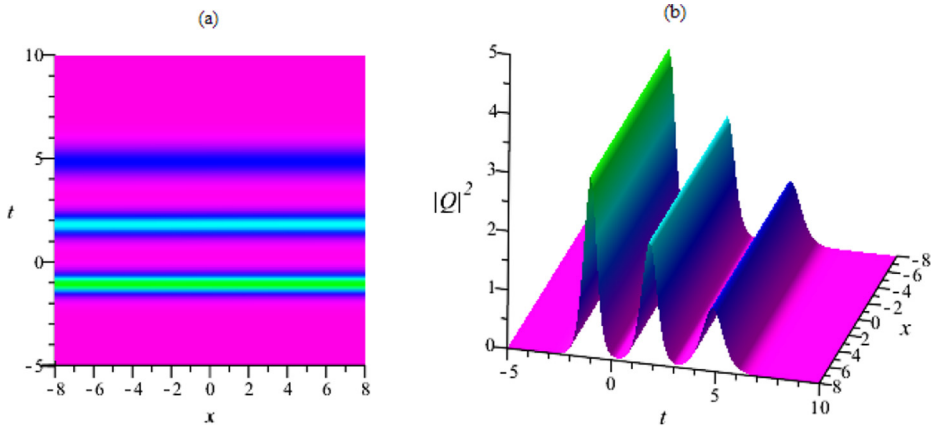

Fig. 6. A soliton molecule consisting of three solitons: (a) density plot and (b) intensity plot. Parameters are $s_{11} = 1.5, s_{12} = -0.3, s_{21} = 2, s_{22} = -0.3, s_{31} = 2.5, s_{32} = -0.3, k_{11} = 0.1, k_{12} = -2, k_{21} = 2, k_{22} = 2, k_{31} = 4, k_{32} = -2, P = 2, \rho(x) = 0, \lambda = 0.5, \alpha(x) = 0.0034\exp(-0.076x)$.

trol the phase shift of the soliton. By changing the parameters of soliton position k_{j1} andk_{j2}, we can change the interval between solitons, but the amplitude of solitons has not changed. In addition, when we change the value of integral constant K, we can only change the amplitude of solitons. When the values of group velocity parameters s_{11} and s_{21} change, the amplitude and phase of soliton will also vary.

Besides the interactions between two soliton, we can also discuss the two-soliton bounded state, currently termed "soliton molecules" [11,12]. Fig. 4 shows a soliton molecule consisting of

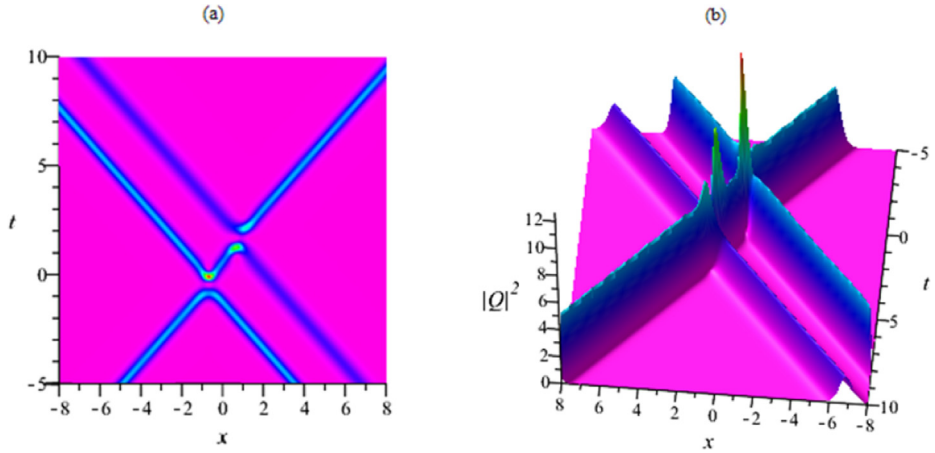

Fig. 7. The interaction of soliton molecules and a bright solitons: (a) density plot and (b) intensity plot. Parameters are$s_{11} = 2, s_{12} = -2, s_{21} = -3, s_{22} = 2, s_{31} = 3, s_{32} = -2, k_{11} = -1, k_{12} = -2, k_{21} = 2, k_{22} = 4, k_{31} = 4, k_{32} = -2, P = 2, \rho(x) = 0, \lambda = 0.5, \alpha(x) = 0.6$.

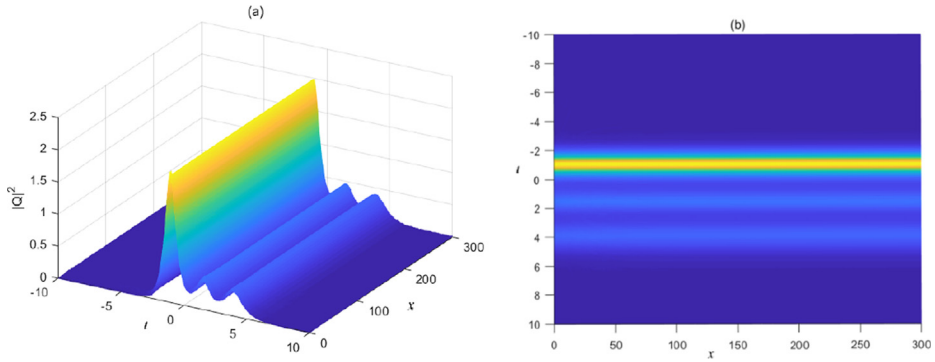

Fig. 8. The numerical rerun of the three-soliton molecule in Fig. 6 with 5% white random noise: (a) intensity plot and (b) density plot. Parameters are $s_{11} = 1.5, s_{12} = s_{22} = s_{32} = -0.3, s_{21} = 2, s_{31} = 2.5, k_{11} = 0.1, k_{12} = k_{32} = -2, k_{21} = k_{22} = 2, k_{31} = 4, P = 2, \rho(x) = 0, \lambda = 0.5, \alpha(x) = 0.0034\exp(-0.076x)$.

two solitons. Recently, Lou et al. gave the velocity resonance conditions of soliton molecules consisting of integer-order solitons in fluid [3,20]. Analyzing two-soliton solution (27), we give the condition of velocity resonance for soliton molecules as $a_{11}(x)/s_{11} = a_{21}(x)/s_{21}$, which means$Im(s_1) = Im(s_2)$. By using the condition of velocity resonance, we can obtain two-soliton molecule. The amplitudes of two soliton in the molecule are different, due tos$_{11} \neq s_{21}$, although their speeds are the same. The distance between the two solitons of the molecule depends on the parameters $k_1$and k_2. If two solitons of the molecule are close enough, the soliton molecule will become an asymmetric soliton, which similar to that in Ref. [48].

In order to analyze the stability of the interaction between two solitons and soliton molecules, we conduct direct numerical rerun for equation (1) using the split-step pulse propagation method. Here the initial field comes from solution (27) with initial 5% white noise. By numerical estimation in Fig. 3(c), we see that two solitons stably propagate a long distance after their interactions. For soliton molecules with$s_{12} = s_{22}$in Fig. 5, two solitons stably form the bounded state a long-distance against the initial 5% white noise. In both evolutionary processes, two solitons have maintained a steady movement.

Furthermore, we can also study the three-soliton molecule, which has the similar velocity resonance condition to the two-soliton molecule. It is easy to know that if the solution (29) satisfies the following resonance conditions as $Im(s_1) = Im(s_2) = Im(s_3)$, namely$s_{12} = s_{22} = s_{32}$, then we can obtain three-solitons molecule. Similarly, we can deduce that if N-solitons satisfies the following resonance conditions $Im(s_1) = Im(s_2) = ...Im(s_n)$, we can obtain N-solitons molecule. In Fig. 6, we can find that the amplitudes of three solitons in the molecule are different owing tos$_{11} \neq s_{21} \neq s_{31}$, although their velocities are the same.

By adjusting the parameterss_{12}, s_{22}, s_{32}, we can study the interaction of two-soliton molecules and a single bright soliton. Fig. 7 exhibits the elastic collision between a molecule consisting of two solitons and a single bright soliton. Due tos$_{11} \neq s_{31}$, the amplitudes of two solitons in the soliton molecule are different, although they have the same speed. Along the propagation distance $\times$, the single bright soliton interacts with the big soliton of the molecule and produces a phase shift, and then interacts with the small soliton of molecule and also appear a phase shift. After the collision, the soliton molecule and the single bright soliton maintain their amplitudes, shapes and widths, which is the elastic interaction. It is known that the collision between the soliton and the soliton in the NLSE is elastic, so the soliton molecule has similar properties as the soliton.

By the numerical rerun in Fig. 8, we see that the three-soliton molecule also stably forms the bounded state a long distance, and maintains good stability. The numerical calculation indicates no collapse, that is, its velocity, shape, amplitude and width are nearly unchanged against the initial 5% white noise.

Conclusions

In conclusion, we consider a fractional NLS equation with distributed coefficients, which describes the propagation of pi-second pulses in inhomogeneous fiber systems. We get analytical chirp-free and chirped non-travelling wave solutions and multi-soliton approximate solutions by two analytical methods, namely, the variable-coefficient fractional mapping method and Hirota method. We give the form conditions of soliton molecules, and study the dynamical characteristics of special fractional solitons, multi-solitons and soliton molecules in the periodic inhomogeneous fiber and the exponentially dispersion decreasing fiber. In the fractional order, the soliton still maintains good stability and forms the bound state of the soliton molecule. An elastic collision occurs between the soliton molecule and the single bright soliton, and their amplitudes, shapes and widths are maintained, and thus soliton molecules have the similar properties as the soliton.

In Figs. 1 and 2, when $\lambda = 1$with the integer case and $\lambda = 0.5$ with the fractional case, the motion effect of soliton is similar, however, the periodicity of the fractional soliton is significantly weakened. In Fig. 3, after the two fractional solitons collide, they keep their original shapes and continue to move. This shows that the fractional order does not affect the properties of integer solitons. Thus the fractional order has a certain effect on the movement of the soliton, but does not change the nature of the soliton. These results have theoretical guidance for the related experimental study in all-optical switches, optical amplifier and mode-locked lasers.

Via the simialr analysis and calculation, we can extend our methods in this paper to two-dimensional FNLS equations and coupled FNLS equations. This will be the direction and focus of our next research.

Declaration of Competing Interest

The authors declare that they have no known competing financial interests or personal relationships that could have appeared to influence the work reported in this paper.

Acknowledgements

This work is supported by the Zhejiang Provincial Natural Science Foundation of China (Grant No. LR20A050001) and the National Natural Science Foundation of China (Grant Nos. 12075210, 11874324, 11775185 and 11975197).

Compliance with ethics requirements

This Research does not involve Human Participants and/or Animals.

Appendix A. Coefficients in solution (29)

$$h_1 = e^{\theta_1} + e^{\theta_2} + e^{\theta_3},$$

$$f_2 = A_1 e^{\theta_1+\theta_1^*} + A_2 e^{\theta_1+\theta_2^*} + A_3 e^{\theta_1+\theta_3^*} + A_4 e^{\theta_2+\theta_1^*} + A_5 e^{\theta_2+\theta_2^*} + A_6 e^{\theta_2+\theta_3^*} + A_7 e^{\theta_3+\theta_1^*} + A_8 e^{\theta_3+\theta_2^*} + A_9 e^{\theta_3+\theta_3^*},$$

$$h_3 = B_1 e^{\theta_1+\theta_1^*+\theta_2} + B_2 e^{\theta_1+\theta_2^*+\theta_2} + B_3 e^{\theta_1+\theta_3^*+\theta_2} + B_4 e^{\theta_1+\theta_1^*+\theta_3} + B_5 e^{\theta_1+\theta_2^*+\theta_3} + B_6 e^{\theta_1+\theta_3^*+\theta_3} + B_7 e^{\theta_2+\theta_1^*+\theta_3} + B_8 e^{\theta_2+\theta_2^*+\theta_3} + B_9 e^{\theta_2+\theta_3^*+\theta_3},$$

$$f_4 = M_1 e^{\theta_1+\theta_1^*+\theta_2+\theta_2^*} + M_2 e^{\theta_1+\theta_1^*+\theta_2+\theta_3^*} + M_3 e^{\theta_1+\theta_3^*+\theta_2+\theta_2^*} + M_4 e^{\theta_1+\theta_1^*+\theta_3+\theta_2^*} + M_5 e^{\theta_1+\theta_1^*+\theta_3+\theta_3^*} + M_6 e^{\theta_1+\theta_2^*+\theta_3+\theta_3^*} + M_7 e^{\theta_3+\theta_1^*+\theta_2+\theta_2^*} + M_8 e^{\theta_3+\theta_1^*+\theta_2+\theta_3^*} + M_9 e^{\theta_3+\theta_3^*+\theta_2+\theta_2^*},$$

$$h_5 = N_1 e^{\theta_1+\theta_1^*+\theta_2+\theta_2^*+\theta_3} + N_2 e^{\theta_1+\theta_1^*+\theta_2+\theta_3^*+\theta_3} + N_3 e^{\theta_1+\theta_3^*+\theta_2+\theta_2^*+\theta_3},$$

$$f_6 = E e^{\theta_1+\theta_1^*+\theta_2+\theta_2^*+\theta_3+\theta_3^*},$$

$$\theta_j = a_j(x) + s_j t + k_j = a_{j1}(x) + i a_{j2}(x) + (s_{j1} + i s_{j2})t + k_{j1} + i k_{j2}, \quad (i = 1, 2, 3),$$

$$a_{j1}(x) = -\Gamma(\lambda+1)\int s_{j1} s_{j2} \alpha(x) dx, a_{j2}(x) = \frac{\Gamma(\lambda+1)}{2}\int (s_{j1}^2 - s_{j2}^2)\alpha(x) dx,$$

$$A_1 = \frac{K}{4s_{11}^2}, A_2 = \frac{K}{d_{31}^2}, A_3 = \frac{K}{d_{32}^2}, A_4 = \frac{K}{d_{21}^2}, A_5 = \frac{K}{4s_{21}^2}, A_6 = \frac{K}{d_{33}^2}, A_7 = \frac{K}{d_{22}^2}, A_8 = \frac{K}{d_{23}^2},$$

$A_9 = \frac{K}{4s_{31}^2}, \beta(x) e^{\frac{2}{\Gamma(\lambda+1)}\int \rho(x) dx} = K\Gamma(\lambda+1)^2 \alpha(x)$,with an arbitrary integration constant K,

$$B_1 = \frac{K d_{11}^2}{4s_{11}^2 d_{21}^2}, B_2 = \frac{K d_{11}^2}{4s_{21}^2 d_{31}^2}, B_3 = \frac{K d_{11}^2}{d_{32}^2 d_{33}^2}, B_4 = \frac{K d_{12}^2}{4s_{11}^2 d_{22}^2}, B_5 = \frac{K d_{12}^2}{d_{31}^2 d_{23}^2}, B_6 = \frac{K d_{12}^2}{4s_{31}^2 d_{32}^2},$$
$$B_7 = \frac{K d_{13}^2}{d_{21}^2 d_{22}^2}, B_8 = \frac{K d_{13}^2}{4s_{21}^2 d_{23}^2}, B_9 = \frac{K d_{12}^2}{4s_{31}^2 d_{33}^2},$$

$$M_1 = \frac{K^2 L_{11}^2}{16 s_{11}^2 s_{21}^2 L_{12}^2}, M_2 = \frac{K^2 d_{11}^2 d_{42}^2}{4 s_{11}^2 d_{21}^2 d_{32}^2 d_{33}^2}, M_3 = \frac{K^2 d_{11}^2 d_{43}^2}{4 s_{21}^2 d_{21}^2 d_{32}^2 d_{33}^2}, M_4 = \frac{K^2 d_{12}^2 d_{41}^2}{4 s_{11}^2 d_{21}^2 d_{22}^2 d_{23}^2},$$
$$M_5 = \frac{K^2 L_{21}^2}{16 s_{11}^2 s_{31}^2 L_{22}^2}, M_6 = \frac{K^2 d_{12}^2 d_{43}^2}{4 s_{31}^2 d_{31}^2 d_{32}^2 d_{23}^2}, M_7 = \frac{K^2 d_{13}^2 d_{41}^2}{4 s_{21}^2 d_{21}^2 d_{22}^2 d_{23}^2}, M_8 = \frac{K^2 d_{13}^2 d_{42}^2}{4 s_{31}^2 d_{21}^2 d_{22}^2 d_{33}^2},$$
$$M_9 = \frac{K^2 L_{31}^2}{16 s_{21}^2 s_{31}^2 L_{32}^2},$$

$$N_1 = \frac{K^2 L_{11}^2 d_{12}^2 d_{13}^2}{16 s_{11}^2 s_{21}^2 d_{21}^2 d_{22}^2 d_{23}^2 d_{31}^2}, N_2 = \frac{K^2 L_{21}^2 d_{11}^2 d_{13}^2}{16 s_{11}^2 s_{31}^2 d_{21}^2 d_{22}^2 d_{32}^2 d_{33}^2}, N_1 = \frac{K^2 L_{31}^2 d_{11}^2 d_{12}^2}{16 s_{21}^2 s_{31}^2 d_{31}^2 d_{32}^2 d_{33}^2 d_{23}^2},$$

$$E = \frac{K^2 L_{11}^2 L_{21}^2 L_{31}^2}{64 s_{11}^2 s_{21}^2 s_{31}^2 d_{21}^2 d_{31}^2 d_{32}^2 d_{33}^2 d_{22}^2 d_{23}^2}$$

$$d_{11} = s_{11} + i s_{12} - s_{21} - i s_{22}, d_{12} = s_{11} + i s_{12} - s_{31} - i s_{32}, d_{13} = s_{21} + i s_{22} - s_{31} - i s_{32},$$

$$d_{21} = s_{11} - i s_{12} + s_{21} + i s_{22}, d_{22} = s_{11} - i s_{12} + s_{31} + i s_{32}, d_{23} = s_{21} - i s_{22} + s_{31} + i s_{32},$$

$$d_{31} = s_{11} + i s_{12} + s_{21} - i s_{22}, d_{32} = s_{11} + i s_{12} + s_{31} - i s_{32}, d_{33} = s_{21} + i s_{22} + s_{31} - i s_{32},$$

$$d_{41} = s_{11} - i s_{12} - s_{21} + i s_{22}, d_{42} = s_{11} - i s_{12} - s_{31} + i s_{32}, d_{43} = s_{21} - i s_{22} - s_{31} + i s_{32},$$

$$L_{11} = (s_{11} - s_{21})^2 + (s_{12} - s_{22})^2, L_{12} = (s_{11} + s_{21})^2 + (s_{12} - s_{22})^2,$$

$$L_{21} = (s_{11} - s_{31})^2 + (s_{12} - s_{32})^2, L_{22} = (s_{11} + s_{31})^2 + (s_{12} - s_{32})^2,$$

$$L_{31} = (s_{21} - s_{31})^2 + (s_{22} - s_{32})^2, L_{32} = (s_{21} + s_{31})^2 + (s_{22} - s_{32})^2.$$

References

[1] Yu WT, Zhou Q, Mirzazadeh M, Liu WJ, Biswas A. Phase shift, amplification, oscillation and attenuation of solitons in nonlinear optics. J Adv Research 2019;15:69–76.
[2] Liu X, Zhou Q, Biswas A, Alzahrani AK, Liu W. The similarities and differences of different plane solitons controlled by (3+1) –dimensional coupled variable coefficient system. J Adv Research 2020;24:167–73.
[3] Yan ZW, Lou SY. Soliton molecules in Sharma–Tasso–Olver–Burgers equation. Applied Mathematics Letters 2020;104:106271.
[4] Dai CQ, Wang YY, Zhang JF. Managements of scalar and vector rogue waves in a partially nonlocal nonlinear medium with linear and harmonic potentials. Nonlinear Dynamics 2020;102:379–91.
[5] Othman MIA, Said SM. 2D problem of magneto-thermoelasticity fiber-reinforced medium under temperature dependent properties with three-phase-lag model. Meccanica 2014;49:1225–43.
[6] Said SM, Othman MIA. Wave propagation in a two-temperature fiber-reinforced magneto-thermoelastic medium with three-phase-lag model. Struct. Eng. and Mech 2016;57:201–20.
[7] Othman MIA, Said SM. The effect of rotation on two-dimensional problem of a fibre-reinforced thermoelastic with one relaxation time. International Journal of Thermophysics 2012;33:160–71.
[8] Liu WJ, Zhu YN, Liu ML, et al. Optical properties and applications for MoS2-Sb2Te3-MoS2 heterostructure materials. Photo. Res. 2018;6:220–7.
[9] Chen YX, Ou-Yang FY. Excitation management of crossed Akhmediev and Ma breather for a nonautonomous partially nonlocal Gross-Pitaevskii equation with an external potential. Nonlinear Dynamics 2020;100:1543–50.
[10] Dai CQ, Wang YY. Coupled spatial periodic waves and solitons in the photovoltaic photorefractive crystals. Nonlinear Dynamics 2020;102:1733–41.
[11] Li PF, Li RJ, Dai CQ. Existence, symmetry breaking bifurcation and stability of two-dimensional optical solitons supported by fractional diffraction. Optics Express 2021;29:3193–209.
[12] Akhmediev N, Ankiewicz A, Soto-Crespo JM. Multisoliton solutions of the complex Ginzburg-Landau equation. Physical Review Letters 1997;6:4047.
[13] Stratmann M, Pagel T, Mitschke F. Experimental observation of temporal soliton molecules. Physical Review Letters 2005;95:143902.
[14] Herink G, Kurtz F, Jalali B, Solli DR, Ropers C. Real-time spectral interferometry probes the internal dynamics of femtosecond soliton molecules. Science 2017;356:50–4.
[15] Lakomy K, Nath R, Santos L. Soliton molecules in dipolar Bose-Einstein condensates. Physical Review A 2012;86:013610.
[16] Krupa K, Nithyanandan K, Andral U, Tchofo-Dinda P, Grelu P. Realtime observation of internal motion within ultrafast dissipative optical soliton molecules. Physical Review Letters 2017;118:243901.
[17] Wang ZQ, Nithyanandan K, Coillet A, Tchofo-Dinda P, Grelu Ph. Optical soliton molecular complexes in a passively mode-locked fibre laser. Nature Commun 2019;10:830.
[18] Peng JS, Boscolo S, Zhao ZH, Zeng HP. Breathing dissipative solitons in mode-locked fiber lasers. Science Advances 2019;5:1110.
[19] Crasovan LC, Kartashov YV, Mihalache D, Torner L, Kivshar YS, Perez-Garcıa VM. Soliton molecules Robust clusters of spatiotemporal optical solitons. Physical Review E 2003;67:046610.
[20] Xu DH, Lou SY. Dark soliton molecules in nonlinear optics. Acta Phys. Sin 2020;69:014208.
[21] Wang B, Zhang Z, Li B. Soliton Molecules and Some Hybrid Solutions for the Nonlinear Schrodinger Equation. Chinese Physics Letters 2020;37:030501.
[22] Kaur B, Gupta RK. Dispersion analysis and improved F-expansion method for space-time fractional differential equations. Nonlinear Dynamics 2019;96:837–52.
[23] Wang BH, Lu PH, Dai CQ, et al. Vector optical soliton and periodic solutions of a coupled fractional nonlinear Schrödinger equation. Results in Physics 2020;17:103036.
[24] A. A. Kilbas, H. M. Srivastava, and J. J. Trujillo, Theory and Applications of Fractional Differential Equations, Amsterdam, 2006.
[25] Fang JJ, Mou DS, Wang YY, Zhang HC, Dai CQ, Chen YX. Soliton dynamics based on exact solutions of conformable fractional discrete complex cubic Ginzburg-Landau equation. Results in Physics 2021;20:103710.
[26] Wang BH, Wang YY, Dai CQ, Chen YX. Dynamical characteristic of analytical fractional solitons for the space-time fractional Fokas-Lenells equation. Alexandria Engineering Journal 2020;59:4699–707.
[27] Othman MIA, Sarkar N, Atwa SY. Effect of fractional parameter on plane waves of generalized magneto–thermoelastic diffusion with reference temperature-dependent elastic medium. Computers & Mathematics with Applications 2013;65:1103–18.
[28] Wang BH, Wang YY. Fractional white noise functional soliton solutions of a wick-type stochastic fractional NLSE. Applied Mathematics Letters 2020;110:106583.
[29] Othman MIA, Said SM, Sarker N. Effect of hydrostatic initial stress and gravity field on a fiber-reinforced thermoelastic medium with fractional derivative heat transfer. Multi. Model. Materials and Struct 2013;9:410–26.
[30] Mehboob AB, Usman M, Hussain Ashiq. Generation and transmission of fractional-order optical bright solitons in singlemode fiber. Microw Opt. Technol. Lett 2019;61:2886–900.
[31] Lu PH, Wang BH, Dai CQ. Fractional traveling wave solutions of the (2 + 1)-dimensional fractional complex Ginzburg-Landau equation via two methods. Math. Meth. Appl. Sci. 2020;43:8518–26.
[32] Sweilam NH, Hasan MMA. Numerical Studies for the Fractional Schrodinger Equation with the Quantum Riesz-Feller Derivative. Progress in Fractional Differentiation and Applications 2016;2:231–45.
[33] N.H. Sweilam, M.M.A. Hasan, et al. Numerical solutions for 2-D fractional Schrodinger equation with the Riesz-Feller derivative. Mathematics and computers in simulation,140 (2017)53-68.
[34] Sweilam NH, Hasan MMA, et al. Numerical solutions of nonlinear fractional Schrdinger equations using nonstandard discretizations. Numerical Methods for Partial Differential Equations 2017;33:1399–419.
[35] Sweilam NH, Hasan MMA. Numerical Simulation for the Variable-Order Fractional Schrdinger Equation with the Quantum Riesz-Feller Derivative. Advances in Applied Mathematics and Mechanics 2017;9:990–1011.
[36] Hashemi MS. Ali Akgül, Solitary wave solutions of time–space nonlinear fractional Schrödinger's equation: Two analytical approaches. Journal of Computational and Applied Mathematics 2018;339:147–60.
[37] Hong B, Lu D, Chen W. Exact and approximate solutions for the fractional Schrodinger equation with variable coefficients. Adv. Diff. Equat 2019;2019:370.
[38] Zhang JF, Dai CQ, Yang Q, Zhu JM. Variable-coefficient F-expansion method and its application to NLSE. Optics Communication 2005;252:408–21.
[39] Liu S, Zhou Q, Biswas A, Liu W. Phase-shift controlling of three solitons in dispersion-decreasing fibers. Nonlinear Dynamics 2019;98:395–401.
[40] Jumarie G. Table of some basic fractional calculus formulae derived from a modified Riemann-Liouville derivative for non-differentiable functions. Applied Mathematics Letters 2009;22:378.
[41] He JH, Elagan SK, Li ZB. Geometrical explanation of the fractional complex transform and derivative chain rule for fractional calculus. Physics Letters A 2012;376:257–9.
[42] El-Sayed AMA, Yousif EA, El-Aasser MA. Analytical solution of the space-time fractional nonlinear Schrödinger equation. Reports on Mathematical Physics 2016;77:19–34.
[43] Hirota R. Exact envelope-soliton solutions of a nonlinear wave equation. Journal of Mathematical Physics 1973;14:805–9.
[44] Sun QH, Pan N, Lei M, Liu WJ. Study on phase-shift control in dispersion decreasing fibers. Acta Phys. Sin. 2014;15:150506.
[45] R.C. Yang, R.Y. H, L. Li, X.J. Shi, Z.H. Li, G.S. Zhou, Exact gray multi-soliton solutions for nonlinear Schrödinger equation with variable coefficients, Optics Communications, 253 (2005) 177–185.
[46] Wang J, Li L, Jia S. Exact chirped gray soliton solutions of the nonlinear Schrodinger equation with variable coefficients. Optics Communication 2007;274:223–30.
[47] Hao RY, Li L, Li ZH, Xue WR, Zhou GS. A new approach to exact soliton solutions and soliton interaction for the nonlinear Schrodinger equation with variable coefficients. Optics Communication 2004;236:79–86.
[48] Lou SY. Soliton molecules and asymmetric solitons in three fifth order systems via velocity resonance. Journal of Physics Communications 2020;4:041002.